

Headline Articles

Synthesis of S^{2-} - and PF_2O_2 -Bridged Dinuclear Ruthenium(IV) Complex Obtained from the Reaction of Disulfide-Bridged Ruthenium(III) Dimer Complex with Dioxygen and Water

Kazuko Matsumoto,* Yoichi Sano, Masaki Kawano, Hiroyuki Uemura, Jun Matsunami, and Toshio Sato†

Department of Chemistry, Advanced Research Center for Science and Engineering, Waseda University, Tokyo 169

†Instrumental Analysis Center of Chemistry, Faculty of Science, Tohoku University, Aramaki Aoba, Aoba-ku, Sendai 980

(Received November 18, 1996)

Reaction of $[\{ Ru(CH_3CN)_3[P(OMe)_3]_2 \}_2(\mu-S_2)](PF_6)_3$ with a mixture of acetylene and O_2 gave a novel ruthenium(IV) dimer complex $[\{ Ru(IV)(PFO_3)[P(OMe)_3]_2 \}_2(\mu-S)(\mu-PF_2O_2)_2]$. The newly formed bridging and terminal ligands $PF_2O_2^-$ and PFO_3^{2-} are produced from the reaction of PF_6^- with trace amounts of H_2O in the solvent. Although acetylene is not incorporated in the final product, it is necessary to accelerate the reaction. Ruthenium(IV) complexes with S^{2-} ligand are rare and only two examples are previously known. The crystal of $[\{ Ru(PFO_3)[P(OMe)_3]_2 \}_2(\mu-S)(\mu-PF_2O_2)_2]$ is monoclinic, space group $P2_1/n$, $a = 11.061(5)$, $b = 20.764(4)$, $c = 17.074(3)$ Å, $\beta = 95.74(2)^\circ$, $V = 3901(1)$ Å³, and $Z = 4$. The bridging $PF_2O_2^-$ ligand coordinates to Ru atoms with the two oxygen atoms, while the terminal PFO_3^{2-} ligand coordinates to a Ru atom with one of the oxygen atoms. The molecular structure is confirmed by ³¹P and ¹⁹F NMR spectroscopy.

We have prepared various dinuclear ruthenium complexes with a disulfide (S_2^{2-}) bridging ligand.^{1–3)} A triply bridged dinuclear complex, $[\{ RuCl[P(OMe)_3]_2 \}_2(\mu-Cl)_2(\mu-S_2)]$ (**1**), loses its bridging and terminal chloride ligands to become $[\{ Ru(an)_3[P(OMe)_3]_2 \}_2(\mu-S_2)]^{n+}$ ($n = 3$ and 4) ($an = CH_3CN$), when reacted with H_2O in AN and Ag^+ in CH_2Cl_2 , respectively.^{2–4)}

The Ru–S–S–Ru core structure in the latter complexes is stable at room temperature but reverts to **1** upon addition of Cl^- to the solution.⁴⁾ Addition of anhydrous hydrazine to **1** leads to the formation of $[\{ RuCl[P(OMe)_3]_2 \}_2(\mu-Cl)(\mu-N_2H_4)(\mu-S_2)]$.³⁾ These reactions suggest that the Ru–S–S–Ru core is suitable to accommodate and possibly to activate substrates by coordination between the two Ru atoms. In the present study, we attempted to react acetylene with $[\{ Ru(an)_3[P(OMe)_3]_2 \}_2(\mu-S_2)](PF_6)_3$ (**2**), however, the reaction was complicated due to the presence of trace amounts of humidity in the solvent, and a very unusual triply bridged dinuclear Ruthenium(IV) complex with one S^{2-} and two $PF_2O_2^-$ bridging ligands, $[\{ Ru[P(OMe)_3]_2(PFO_3) \}_2(\mu-S)(\mu-PF_2O_2)_2]$ (**3**), was obtained.

Experimental

The starting complex **2** was prepared from **1** according to a

slightly modified method in Ref. 2, as described in the following paragraph. Diethyl ether was dried with $CaCl_2$, and distilled in the presence of benzophenone and sodium metal. Analytical reagent grade acetonitrile was used as purchased. Dichloromethane of a low-water-content grade (water less than 0.003%, Kokusan Chemicals Co.) was used as purchased without purification. Commercially available dissolved acetylene was first bubbled through concd H_2SO_4 , and was condensed in a trap immersed in liq. N_2 . The acetylene gas was vaporized by transferring the trap into a dry ice–methanol bath, and was introduced into the reaction vessel.

A Modified Preparative Method for 2. To 50 cm³ of CH_3CN containing 0.90 g (1 mmol) of **1** was added 100 cm³ of H_2O containing 1.01 g (6 mmol) of $NaPF_6$. The solution became pale green, and blue microcrystals appeared after stirring for 5 to 6 h at room temperature. The crystals were filtered, recrystallized from CH_2Cl_2 , vacuum-dried, and were stored under N_2 . The compound was confirmed by elemental analysis. The yield was 75%.

Preparation of 3. Compound **2** (0.05 g, 4.4×10^{-2} mmol) was dissolved into 15 cm³ of commercial reagent grade CH_2Cl_2 in a Schlenk bottle, to which a mixture of 400 cm³ of acetylene and 100 cm³ of O_2 in a balloon was added. The solution was stirred at room temperature for 2 d, during which time the blue color of the solution darkened, and finally changed to violet. The solution was concentrated to 5 cm³, and 35 cm³ of Et_2O was added to give microcrystals of **3**. The crystals were recrystallized from 5 cm³ of CH_2Cl_2 and 35 cm³ of Et_2O 2 to 3 times. Crystals suitable for X-

ray work were obtained after 1 week by two-pot ether diffusion to the CH_2Cl_2 solution at 0°C . The yield was 20%. Compound **3** is not stable in air, and must be stored under dry N_2 . Anal. Calcd for $\text{C}_{12}\text{F}_6\text{H}_{36}\text{O}_{22}\text{P}_8\text{Ru}_2\text{S}$ (F.W. = 1128.39): C, 12.77; H, 3.22%. Found: C, 13.15; H, 3.39%. UV-vis (CH_2Cl_2) 547 (5820), 439 (894), 347 (6060), 270 nm ($16900\text{ mol}^{-1}\text{ dm}^3\text{ cm}^{-1}$).

Collection and Reduction of X-Ray Data. A crystal of **3** was subjected to single-crystal X-ray diffraction analysis. The crystal ($0.25 \times 0.30 \times 0.35\text{ mm}^3$) was coated with epoxide-resin and was used for measurement. Unit cell parameters were obtained from a least-squares fit of 25 reflections in the range $23^\circ < 2\theta < 25^\circ$ measured on a Rigaku AFC-7R four circle diffractometer by using monochromated $\text{Mo K}\alpha$ radiation. The Lorentz-polarization correction and empirical absorption correction were made to the collected data. Atomic scattering factors and anomalous dispersion correction were taken from Ref. 5. The crystal data are given in Table 1.

Solution and Refinement of the Structure. The coordinates of Ru, S, and P atom were found by a direct method, and a series of full-matrix least-squares refinements followed by Fourier synthesis (teXsan) revealed all the remaining atoms except hydrogen atoms. The structure was finally refined with anisotropic temperature factors for all the atoms to the final discrepancy index of $R = 0.039$ and $R_w = 0.042$, where $R = \Sigma(|F_o| - |F_c|)/\Sigma|F_o|$ and $R_w = [\Sigma w_i(|F_o| - |F_c|)^2/\Sigma w_i|F_o|^2]^{1/2}$ ($w_i = 1/\sigma(F)^2$). The final positional and thermal parameters are listed in Table 2. The $F_o - F_c$ data are deposited as Document No. 70017 at the Office of the Editor of

Bull. Chem. Soc. Jpn.

Physical Measurements. $^{31}\text{P}\{^1\text{H}\}$ NMR spectra were recorded on a JEOL EX270WB instrument, whereas ^{19}F NMR spectra were on a GE OMEGA 500 instrument. The chemical shifts are expressed in ppm, and are referenced to an external standard of 85% H_3PO_4 for ^{31}P and NaPF_6 for ^{19}F . FAB mass spectra were obtained on a JEOL JMS-HX110 mass spectrometer with a sample of a nitrobenzyl alcohol solution.

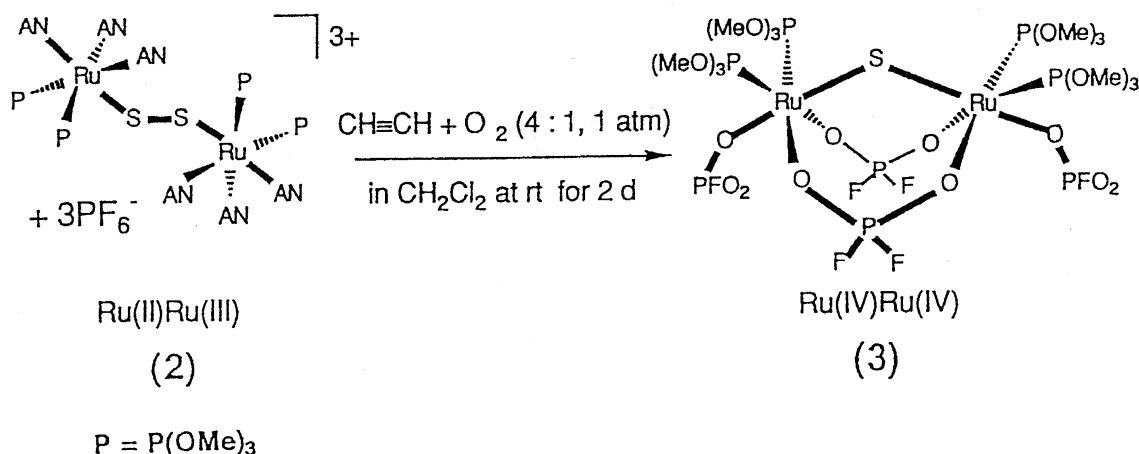
Results and Discussion

Preparation of 3. The reaction of **2** with acetylene and O_2 is expressed in Scheme 1. Although the product **3** does not contain acetylene, addition of acetylene facilitates the reaction; addition of only O_2 leads to a very gradual color change, resulting in formation of a dark blue solution, from which **3** was obtained in less yield. The reaction without acetylene needs more than a week to obtain a substantial amount of **3**. Addition of only acetylene, in contrast, did not lead to appreciable reaction. Addition of both acetylene and O_2 accelerates the reaction and finally gives **3**. The reaction needs fairly dry conditions, but trace amounts of water are necessary. An excess amount of water disturbs the reaction and only dark brown oily material is obtained. The bridging ligand PF_2O_2^- is known to be unstable toward humidity,⁶ which explains why the reaction has to be done under dry

Table 1. Crystal Data for $[\{\text{Ru}(\text{PFO}_3)[\text{P}(\text{OMe})_3]_2\}_2(\mu\text{-PO}_2\text{F}_2)_2(\mu\text{-S})]$

Formula	$\text{C}_{12}\text{F}_6\text{H}_{36}\text{O}_{22}\text{P}_8\text{Ru}_2\text{S}$	Z	4
Formula weight	1128.4	$D_{\text{calcd}}/\text{g cm}^{-3}$	1.92
		Abs. coeff (μ)/ cm^{-1}	13.13
Crystal system	Monoclinic	Radiation ($\lambda/\text{\AA}$)	0.71069
Space group	$P2_1/n$ (No. 14)	R^a	0.039
$a/\text{\AA}$	11.061(5)	R_w^b	0.042
$b/\text{\AA}$	20.764(4)	($w = 1/\sigma(F)^2$)	
$c/\text{\AA}$	17.074(3)	GOF ^c	1.89
β/deg	95.74(2)	$T/^\circ\text{C}$	
$V/\text{\AA}^3$	3901(1)	No. of reflns measd	9688
		No. of reflns used	5604

a) $R = \Sigma(|F_o| - |F_c|)/\Sigma|F_o|$. b) $R_w = [\Sigma w(|F_o| - |F_c|)^2/\Sigma w|F_o|^2]^{1/2}$. c) $\text{GOF} = [\Sigma w(|F_o| - |F_c|)^2/\Sigma|N_{\text{reflens}} - N_{\text{params}}|]^{1/2}$.



Scheme 1.

Table 2. Atomic Coordinates and Equivalent Isotropic Temperature Factors (\AA^2) for $[\{\text{Ru}(\text{PFO}_3)[\text{P}(\text{OMe})_3]_2\}_2(\mu\text{-P}_2\text{O}_7)_2(\mu\text{-S})]$

Atom	<i>x</i>	<i>y</i>	<i>z</i>	<i>B</i> _{eq}
Ru(1)	0.48100(4)	0.20484(2)	0.86348(3)	2.245(10)
Ru(2)	0.61683(4)	0.35560(2)	0.81223(3)	2.380(10)
S(1)	0.4708(1)	0.28714(7)	0.78588(8)	2.49(3)
P(1)	0.7789(1)	0.22927(8)	0.85773(10)	3.00(4)
P(2)	0.5851(1)	0.30518(8)	0.99638(9)	2.83(3)
P(3)	0.5700(2)	0.10704(9)	1.01717(10)	3.55(4)
P(4)	0.8768(2)	0.42113(9)	0.8959(1)	4.03(4)
P(5)	0.4834(1)	0.14190(8)	0.75578(9)	2.92(3)
P(6)	0.2777(1)	0.19770(9)	0.85087(10)	3.18(4)
P(7)	0.6054(1)	0.37993(8)	0.68386(9)	2.94(4)
P(8)	0.4800(2)	0.43375(8)	0.83230(10)	3.24(4)
F(1)	0.8386(3)	0.1752(2)	0.8113(2)	4.63(10)
F(2)	0.8839(3)	0.2461(2)	0.9225(2)	6.0(1)
F(3)	0.6754(4)	0.2715(2)	1.0587(2)	5.5(1)
F(4)	0.5298(3)	0.3571(2)	1.0474(2)	4.50(9)
F(5)	0.5030(5)	0.0545(2)	1.0592(2)	6.6(1)
F(6)	0.8430(60)	0.4678(3)	0.9600(3)	11.1(2)
O(1)	0.6745(3)	0.1986(2)	0.8919(2)	2.86(9)
O(2)	0.7546(3)	0.2840(2)	0.8017(2)	3.06(9)
O(3)	0.4829(3)	0.2615(2)	0.9682(2)	2.82(9)
O(4)	0.6504(3)	0.3400(2)	0.9371(2)	2.97(9)
O(5)	0.4905(4)	0.1239(2)	0.9454(2)	3.29(10)
O(6)	0.6757(4)	0.0663(2)	0.9935(3)	4.8(1)
O(7)	0.6159(4)	0.1545(2)	1.0764(2)	4.4(1)
O(8)	0.7739(4)	0.4193(2)	0.8351(2)	3.7(1)
O(9)	0.9329(4)	0.3652(2)	0.9353(3)	5.3(1)
O(10)	0.9725(4)	0.4627(3)	0.8659(3)	7.6(2)
O(11)	0.5952(5)	0.1607(3)	0.7097(3)	6.5(2)
O(12)	0.4905(4)	0.0668(2)	0.7679(3)	4.7(1)
O(13)	0.3697(4)	0.1483(2)	0.6935(4)	4.5(1)
O(14)	0.2219(4)	0.1281(2)	0.8326(3)	4.9(1)
O(15)	0.2154(4)	0.2398(2)	0.7821(3)	4.2(1)
O(16)	0.2134(4)	0.2140(3)	0.9265(3)	5.3(1)
O(17)	0.6869(4)	0.3408(2)	0.6306(3)	4.7(1)
O(18)	0.4790(4)	0.3724(2)	0.6341(2)	4.1(1)
O(19)	0.6350(4)	0.4536(2)	0.6723(2)	4.4(1)
O(20)	0.4102(4)	0.4133(2)	0.9036(3)	4.7(1)
O(21)	0.3805(4)	0.4560(2)	0.7649(3)	4.6(1)
O(22)	0.5350(5)	0.5012(2)	0.8596(3)	5.5(1)
C(1)	0.617(1)	0.1447(6)	0.6341(6)	9.8(4)
C(2)	0.5990(8)	0.0351(4)	0.8037(4)	6.1(2)
C(3)	0.3168(9)	0.1006(4)	0.6405(5)	8.6(3)
C(4)	0.2125(10)	0.0781(5)	0.8880(6)	9.2(3)
C(5)	0.0857(6)	0.2382(5)	0.7559(5)	6.4(2)
C(6)	0.2088(7)	0.2797(5)	0.9556(5)	6.8(3)
C(7)	0.8198(6)	0.3378(5)	0.5750(5)	7.2(3)
C(8)	0.6228(8)	0.4844(4)	0.5947(4)	6.7(2)
C(9)	0.3226(8)	0.4573(4)	0.9441(5)	6.5(1)
C(10)	0.2710(6)	0.4181(4)	0.7386(5)	5.7(2)
C(11)	0.5741(9)	0.5515(4)	0.8087(5)	7.1(3)

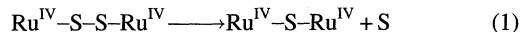
$$B_{\text{eq}} = 8/3\pi^2 (U_{11}(aa^*)^2 + U_{22}(bb^*)^2 + U_{33}(cc^*)^2 + 2U_{12}aa^*bb^*\cos\gamma + 2U_{13}aa^*cc^*\cos\beta + 2U_{23}bb^*cc^*\cos\alpha).$$

conditions. Complex **3** is unstable toward humidity and should be kept under dry N_2 .

Although PF_6^- is usually believed to be very stable,⁷⁾ it is known to undergo hydrolysis to PF_2O_2^- and PFO_3^{2-} in the presence of various acids and aquametal complexes.⁸⁾ The

ligands PF_2O_2^- and PFO_3^{2-} in **3** have been produced by hydrolysis as the $^{18}\text{O}_2$ experiment and mass spectrometric studies show: Complex **3** synthesized with $^{18}\text{O}_2$ showed no significant difference from the result obtained with $^{16}\text{O}_2$. Therefore, the oxygen atoms in **3** originate from trace amounts of water in the solvent. In accordance with this, the best solvent for the preparation of **3** was found to be commercially available reagent-grade CH_2Cl_2 rather than low-water-content grade or laboratory-distilled CH_2Cl_2 . However, the reaction is disturbed, if the solvent contains excess water; **3** cannot be obtained in CH_2Cl_2 with a drop of water. In this regard, the reaction time for **3** is critical to the synthesis; if the reaction time is more than 2 d, **3** cannot be obtained, since hydrolytic degradation is caused by the excess water.

Acetylene obviously accelerates the reaction, but its role is unknown. It is plausible that acetylene reacts with the bridging S_2^{2-} to remove one sulfur atom, although no such reaction is known for free sulfur S_8 and unsubstituted acetylene. It is widely known that acetylene derivatives easily react with S_8 to give cyclic addition products including thiophen derivatives.⁹⁾ We examined the reaction solution by gas-chromatography for possible existence of thiophen, but it was not detected. Unsubstituted acetylene and S_8 react to give unidentified products.⁹⁾ Another plausible explanation of the role of acetylene is that acetylene reacts with elemental sulfur, which is produced by spontaneous reaction of the disulfide-bridged ruthenium(IV) dimer (Eq. 1), thus accelerating the reaction.



The disulfide-bridged ruthenium(IV) dimer in Eq. 1 is expected to be produced by O_2 oxidation of **2**. Reaction (1) is reported for $[\{\text{Ru}^{\text{IV}}(\text{Hedta})\}(\mu\text{-S}_2)]$ upon refluxing a 1 : 1 water–ethanol solution for 8–10 h.¹⁰⁾

Structure of Complex 3. The structure of complex **3** and the atomic numbering scheme is shown in Fig. 1. The distinction between F and O atoms, which was not possible

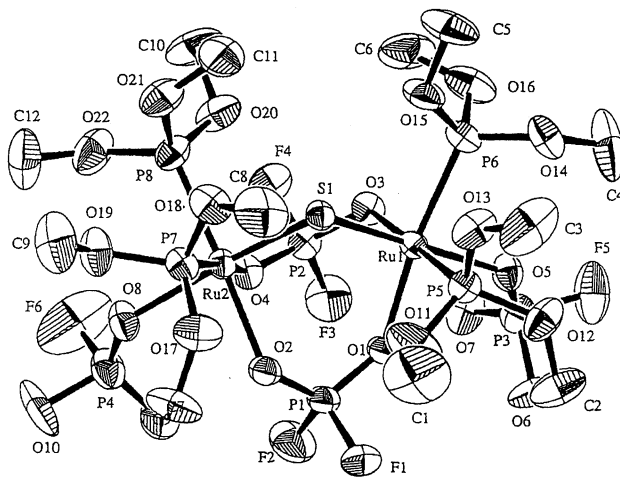


Fig. 1. Molecular structure of $[\{\text{Ru}(\text{P}(\text{OMe})_3)_2(\text{PFO}_3)_2\}_2(\mu\text{-S})(\mu\text{-PF}_2\text{O}_2)_2]$ (**3**). The thermal ellipsoids are drawn at 30% probability.

only with X-ray analysis, was carried out with the aid of elemental analysis and ^{31}P and ^{19}F NMR spectra, as detailed later. All the bond distances around the Ru atoms are listed in Table 3.

It is noteworthy that the original S_2^{2-} bridge in the starting material **2** has been reduced to S^{2-} in **3**. Ruthenium complexes with bridging S^{2-} ligand(s) are very rare; **3** is the third S^{2-} -bridged ruthenium complex, as far as the authors know, the first being Ru-S cubane complex $[\text{Ru}_4^{\text{III,IV}}(\text{CpMe})_4\text{S}_4]$ (CpMe is methylcyclopentadienide),¹¹⁾ and the second, $[\{\text{Ru}^{\text{IV}}(\text{Hedta})\}_2(\mu\text{-S})]$ (H_4edta =ethylenediaminetetraacetic acid). The Ru-S distances in **3** (2.158(2) and 2.165(2) Å) are significantly shorter than those in the reported disulfide (S_2^{2-}) bridged ruthenium(III) dimer complexes (2.193–2.360 Å).^{1–3,12–18)} Furthermore, the Ru-S distances in **3** are shorter even than those in the sulfide-bridged cubane complex $[\text{Ru}_4(\text{CpMe})_4\text{S}_4]$ (2.300–2.379 Å),¹¹⁾ in which Ru atoms are in a ruthenium(III, IV) mixed-valent state.

^{31}P and ^{19}F NMR Spectroscopy. Complex **3** is stable in CH_2Cl_2 and can be recrystallized from the solution. Since the F and O atoms in the PF_2O_2^- and PFO_3^{2-} ligands could not be determined unambiguously by only X-ray diffraction analysis, the ^{31}P and ^{19}F NMR spectra in CD_2Cl_2 were measured; results are shown in Fig. 2. The temperature dependence of the PFO_3^{2-} and PF_2O_2^- region in the ^{19}F and ^{31}P spectra are shown in Figs. 3 and 4, respectively.

The ^{31}P and ^{19}F NMR spectra in Fig. 2 show that the ^{31}P signal of PF_2O_2^- is split into a triplet (−7.24, −15.86, and −24.48 ppm) with $^1J_{\text{PF}}=943$ Hz, whereas PFO_3^{2-} exhibits a doublet ^{31}P signal with $^1J_{\text{PF}}=879$ Hz. Each of the two lines in the doublet consists of a quintet (−0.09, −0.16, −0.25, −0.33, −0.40, −8.13, −8.21, −8.30, −8.37, and −8.45 ppm). The reasons for the split will be detailed later. The ^{19}F spectrum in Fig. 2 shows two sets of doublets for PF_2O_2^- and PFO_3^{2-} , each with a $^1J_{\text{PF}}$ value corresponding to that observed in the respective ^{31}P signal. Each line of the doublet for PFO_3^{2-} is further split into a close-lying quintet (−77.36, −77.37, −77.38, −77.39, −77.40, −79.23, −79.24, −79.25, −79.26, and −79.27 ppm); the reason for the split will be explained later.

It is not possible only from the room temperature ^{31}P and ^{19}F spectra to determine which of the PFO_3^{2-} and PF_2O_2^- ligand is bridging and which of the two is the terminal ligand. On lowering the temperature, the ^{19}F signal of PF_2O_2^- gradually becomes a second-order ABX pattern (Fig. 3). This

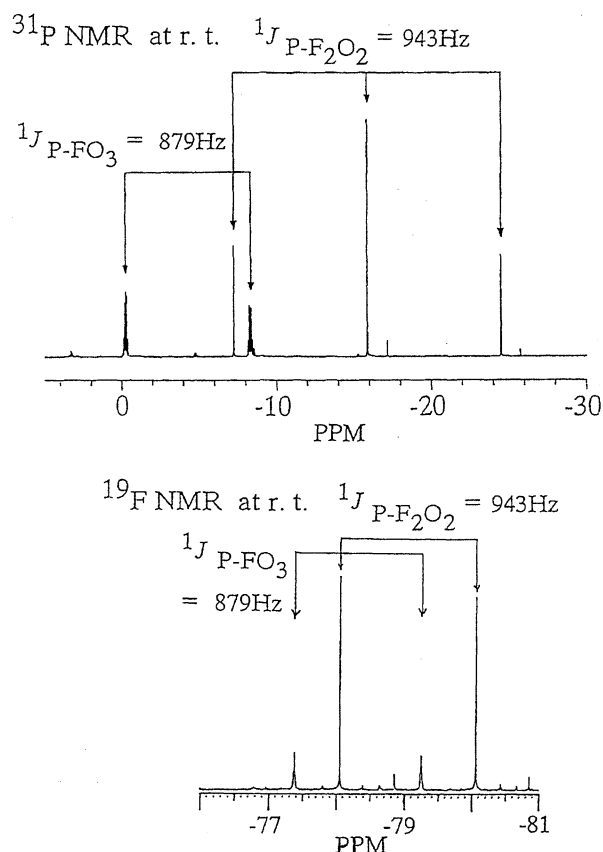


Fig. 2. ^{31}P and ^{19}F NMR spectra of **3** in CD_2Cl_2 at room temperature.

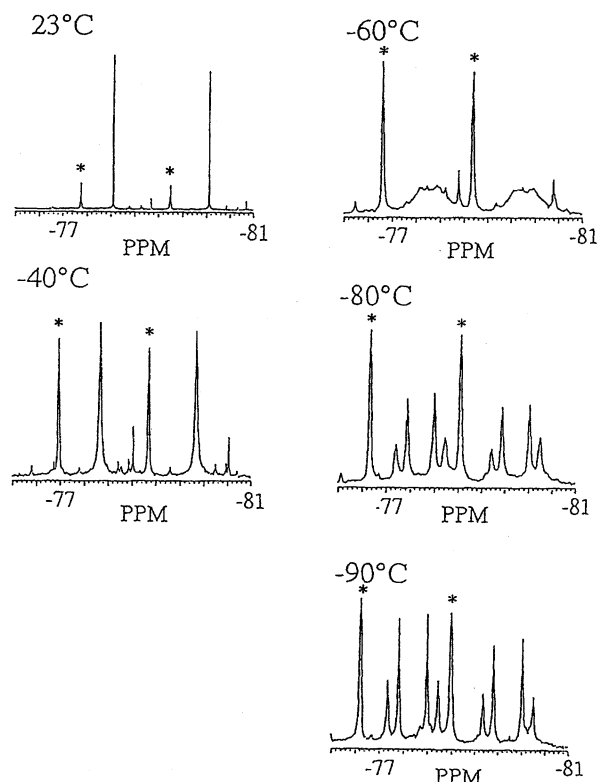


Fig. 3. Variable temperature ^{19}F spectra of **3** for the PFO_3^{2-} and PF_2O_2^- region. The asterisks denote the peaks for PFO_3^{2-} .

Table 3. Bond Lengths (Å) for $[\{\text{Ru}(\text{PFO}_3)[\text{P}(\text{OMe})_3]_2\}_2(\mu\text{-PO}_2\text{F}_2)_2(\mu\text{-S})]$

Atom	Distance	Atom	Distance
Ru(1)–S(1)	2.158(2)	Ru(1)–P(5)	2.258(2)
Ru(1)–P(6)	2.243(2)	Ru(1)–O(1)	2.151(4)
Ru(1)–O(3)	2.138(4)	Ru(1)–O(5)	2.183(4)
Ru(2)–S(1)	2.165(2)	Ru(2)–P(3)	2.240(2)
Ru(2)–P(4)	2.268(2)	Ru(2)–O(2)	2.150(4)
Ru(2)–O(4)	2.188(4)	Ru(2)–O(6)	2.151(4)

suggests that PF_2O_2^- is the bridging ligand, and the two F atoms are equivalent at room temperature due to a large thermal flapping motion. This, however, is frozen out at -90°C and the two F atoms become inequivalent with one being axial (F_a) and the other equatorial (F_e) (see Fig. 4). The chemical shifts of ^{19}F at -90°C are -76.61 , -77.19 , -77.40 , -77.99 , -78.22 , -78.50 , -79.16 , -79.40 , -80.00 , and -80.23 ppm. The corresponding temperature dependence of the ^{31}P signals of PF_2O_2^- , PFO_3^{2-} , and $\text{P}(\text{OMe})_3$ are shown in Figs. 4 and 5. The chemical shifts of ^{31}P at -90°C are 126.01 , 124.01 , 116.00 , 113.99 , -0.18 , -0.25 , -0.33 , -7.24 , -8.21 , -8.28 , -8.37 , -15.86 , and -24.48 ppm.

The lack of coupling of the PF_2O_2^- to $\text{P}(\text{OMe})_3$ ligand at room temperature can be explained by the large flapping motion of PF_2O_2^- . Such flapping of a bridging PF_2O_2^- ligand is also reported for $[(\text{C}_5\text{Me}_5)\text{Rh}(\text{PO}_2\text{F}_2)_3\text{Rh}(\text{C}_5\text{Me}_5)]^+$, where coupling between the Rh and F atoms is not observed.¹⁹⁾

PFO_3^{2-} is determined to be terminal coordination, since its ^{19}F variable temperature spectrum (Fig. 3) shows no further significant shift, broadening, or splitting of the peaks on lowering the temperature to -90°C . Each of the ^{31}P NMR doublet signals of PFO_3^{2-} is actually a five-line quasi-quintet ($J=9.1$ Hz) at room temperature and seems to be a triplet at -90°C . The ^{31}P and ^{19}F nuclei of PFO_3^{2-} and PF_2O_2^- are not coupled to each other. This is manifested by the fact that the spectra do not have any splitting caused by the

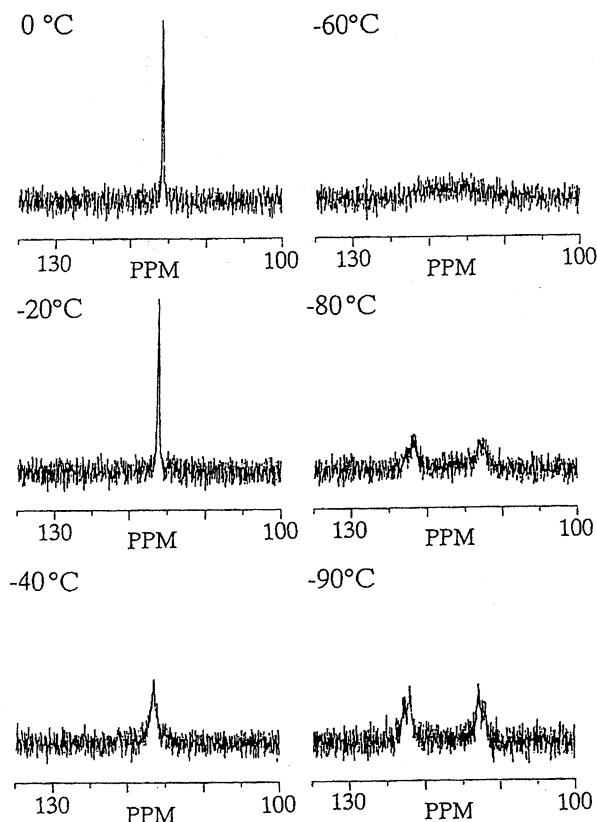


Fig. 5. Variable temperature ^{31}P spectra of **3** for the $\text{P}(\text{OMe})_3$ region.

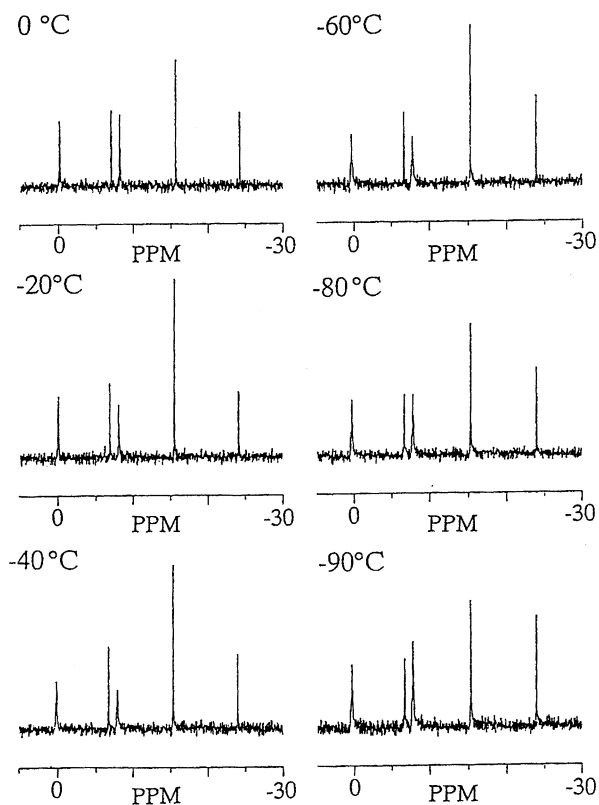


Fig. 4. Variable temperature ^{31}P spectra of **3** for the PFO_3^{2-} and PF_2O_2^- region.

coupling between PFO_3^{2-} and PF_2O_2^- . The quintets of ^{31}P and ^{19}F of PFO_3^{2-} at room temperature are both due to the coupling to $\text{P}(\text{OMe})_3$, which is supported by the broadening (half-width of 22.3 Hz) of the ^{31}P signal of $\text{P}(\text{OMe})_3$. The ^{31}P and ^{19}F quintet signals can be explained by assuming that three different environments exist for the $\text{P}(\text{OMe})_3$ ligands, although the actual difference of the environments is unknown. The quintet can be considered as an overlap of three sets of triplets (Fig. 6). Each triplet is brought about by the two equivalent $\text{P}(\text{OMe})_3$ ligands. In accordance with this explanation, the ^{31}P signal of $\text{P}(\text{OMe})_3$ is broad (22.3 Hz). This is caused by its coupling to ^{31}P and ^{19}F of PFO_3^{2-} with coupling constants of 8.9 and 4.9 Hz, respectively; note that the calculated half-width for $\text{P}(\text{OMe})_3$ is ca. 20 Hz, which is in good agreement with the experimental value. At -90°C ,

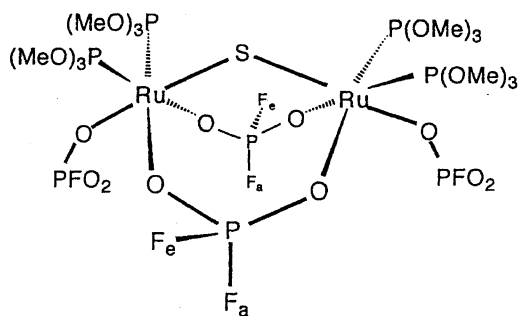


Fig. 6. A scheme of the ligand bonding orientations in **3**.

the two $\text{P}(\text{OMe})_3$ ligands become inequivalent, thus being split into a doublet. At this temperature, the ^{31}P signal of PFO_3^{2-} is a triplet, since the structure of the ligand is probably frozen on the NMR time scale in the form found in the crystal structure (Fig. 1), and the ^{31}P signal is observed as an overlap of two doublets as explained earlier.

The present study is financially supported by a Grant-in-Aid for Scientific Research on Priority Areas of "Activation of Small Molecules" No. 04241225 and "Reactive Organometallics" No. 05236104 from the Ministry of the Education, Science, Sports and Culture.

References

- 1) T. Matsumoto and K. Matsumoto, *Chem. Lett.*, **1992**, 559.
- 2) T. Matsumoto and K. Matsumoto, *Chem. Lett.*, **1992**, 1539.
- 3) M. Kawano, C. Hoshino, and K. Matsumoto, *Inorg. Chem.*, **31**, 5158 (1992).
- 4) K. Matsumoto, T. Matsumoto, M. Kawano, H. Ohnuki, Y. Shichi, T. Nishide, and T. Sato, *J. Am. Chem. Soc.*, **118**, 3597 (1996).
- 5) a) D. T. Cramer and J. T. Waber, "International Tables for X-Ray Crystallography," Kynoch Press, Birmingham, England (1974), Vol. IV, p. 71; b) D. C. Creagh and W. J. McAuley, "International Tables for Crystallography," Kluwer Academic Publishers, Boston (1992), Vol. C, p. 219.
- 6) H. R. Clark and M. M. Jones, *Inorg. Chem.*, **10**, 28 (1971).
- 7) a) A. E. Gebala and M. M. Jones, *J. Inorg. Nucl. Chem.*, **31**, 771 (1969); b) W. Lange, *Ber. Dtsch. Chem. Ges.*, **61**, 799 (1928).
- 8) a) G. I. Ryss and V. B. Tul'chinskii, *Zh. Neorg. Khim.*, **9**, 836 (1967); b) H. R. Clark and M. M. Jones, *J. Am. Chem. Soc.*, **92**, 816 (1970); c) H. Bauer, U. Nagel, and W. Beck, *J. Organomet. Chem.*, **290**, 219 (1985); d) E. Horn and M. R. Snow, *Aust. J. Chem.*, **33**, 2369 (1980).
- 9) J. Nakayama, K. Akimoto, and M. Hoshino, *Rev. Heteroatom Chem.*, **3**, 146 (1990).
- 10) M. M. T. Khan and M. R. H. Siddiqui, *Inorg. Chem.*, **30**, 1157 (1991).
- 11) J. Amarasekera, T. B. Rauchfuss, and S. R. Wilson, *J. Chem. Soc., Chem. Commun.*, **1989**, 14.
- 12) K. Matsumoto, H. Uemura, and M. Kawano, *Inorg. Chem.*, **34**, 658 (1995).
- 13) J. Amarasekera, T. B. Rauchfuss, and S. R. Wilson, *Inorg. Chem.*, **26**, 3328 (1987).
- 14) R. C. Elder and M. Trkula, *Inorg. Chem.*, **16**, 1048 (1977).
- 15) D. Sellmann, P. Lechner, F. Knoch, and M. Moll, *J. Am. Chem. Soc.*, **114**, 922 (1992).
- 16) J. Amarasekera, T. B. Rauchfuss, and A. L. Rheingold, *Inorg. Chem.*, **26**, 2017 (1987).
- 17) Y. Mizobe, M. Hosomizu, J. Kawabata, and M. Hidai, *J. Chem. Soc., Chem. Commun.*, **1991**, 1226.
- 18) T. B. Rauchfuss, D. P. S. Rodgers, and S. R. Wilson, *J. Am. Chem. Soc.*, **108**, 3114 (1986).
- 19) S. J. Thompson, P. M. Bailey, C. White, and P. M. Maitlis, *Angew. Chem., Int. Ed. Engl.*, **15**, 490 (1976).